Journal of Thermal Analysis and Calorimetry, Vol. 58 (1999) 257-267

THERMAL DECOMPOSITION MECHANISM, THERMODYNAMICAL AND QUANTUM CHEMICAL OF PROPERTIES [$Pb(NTO)_2 \cdot (H_2O)$]

S. Jirong[1], *C. Zhaoxu*[2], *Hu Rongzu*[3*], *X. Heming*[2] *and L. Fuping*[3]

[1]Department of Chemical Engineering, Northwest University, Xi'an 710069, Shaanxi
[2]Department of Chemical, Nanjing University of Science and Technology, Nanjing 210094
[3]Xi'an Modern Chemistry Research Institute, Xi'an 710065, Shaanxi, P. R. China

Abstract

The single crystal of lead salt of 3-nitro-1,2,4-triazol-5-one (NTO), [$Pb(NTO)_2 \cdot H_2O$] was prepared and its structure was determined by a four-circle X-ray diffractometer. The crystal is monoclinic, its space group is $P2_1/n$ with crystal parameters of a=0.7262(1) nm, b=1.2129(2) nm, c=1.2268(3) nm, β=90.38(2)°, V=1.0806(2) nm^3, Z=4, D_c=2.97 g cm^{-3}, μ=157.83 cm^{-1}, $F(000)$=888. The final R is 0.027. By using SCF-PM3-MO method we obtained optimized geometry for [$Pb(NTO)_2 \cdot H_2O$] and particularly positions for hydrogen atoms. Through the analyses of MO levels and bond orders it is found that Pb atom bond to ligands mainly with its $6p_z$ and $6p_y$ AOs. The thermal decomposition experiments are elucidated when [$Pb(NTO)_2 \cdot H_2O$] is heated, ligand water is dissociated first and NO_2 group has priority of leaving. Based on the thermal analysis, the thermal decomposition mechanism of [$Pb(NTO)_2 \cdot H_2O$] has been derived. The lattice enthalpy and its lattice energy were also estimated.

Keywords: crystal structure, lattice energy, lattice enthalpy, lead salt of NTO, preparation, quantum chemical calculation, thermal decomposition mechanism

Introduction

Much attention has been paid to 3-nitro-1,2,4-triazol-5-one (NTO) as a high energy and low sensitivity energetic material [1, 2]. Its metal salts also have some potential uses in ammunition [3–7], especially its lead salt as a catalyst.

Therefore, the authors prepared the single crystal of [$Pb(NTO)_2 \cdot H_2O$], determined its structure, studied its thermal decomposition mechanism and thermodynamic properties and made a quantum chemical calculation.

Experimental

Materials

[$Pb(NTO)_2 \cdot H_2O$] used in this research work was prepared according to the following method: An appropriate amount of NTO was put into the distilled water

* Author to whom all correspondence should be addressed.

1418–2874/99/ $ 5.00

Akadémiai Kiadó, Budapest
Kluwer Academic Publishers, Dordrecht

(M:V=1:4), then stirred and titrated with aqueous solution of sodium hydroxide under 60°C until pH reached 6–7. The prepared solution was gradually dropped to an aqueous solution of lead nitrate at 60°C, then stirred and heated at 60°C for 30 min to get yellow precipitates. The precipitate was recrystallized with distilled water at the culture box of 25°C to obtain yellow single crystal for X-ray measurement. Dimensions of the single crystal were $0.1\times0.105\times0.12$ mm^3.

Experimental equipment and conditions

In the determination of the structure of single crystal, X-ray intensities were recorded by a CAD4PDP11/44 automatic diffractometer with graphite-monochromatized MoK_α radiation, λ=0.071073 nm. Cell parameters were determined from 25 reflections. Data collected by $\omega/2\theta$ scan mode in the range of $2^\circ\leq\theta\leq25^\circ$, h=0–8, k=0–14, l=–14 – +14, and 1881 independent reflections were got, among which 1593 with $I>3\sigma(I)$, were used for the determination and refinement of crystal structure. Lorentz-polarization and absorption correction was applied. The coordinates of Pb atom were obtained by Patterson method and those of the other atoms were got by difference Fourier syntheses. Refinement was performed by block-diagonal least-square methods using anisotropic thermal parameters for non-hydrogen atoms, fixed thermal parameters for hydrogen atoms. All calculations were carried out with SDP program on a PDP11/44 computer.

The thermal decomposition process was studied using a TG technique on a Delta Series TGA 7 (Perkin Elmer Co., USA). The conditions of TG were as follows: sample mass about 1 mg, heating rate 10°C min^{-1}; atmosphere flowing N_2/O_2 mixture (with a ratio in air). The DSC experiments were carried out with a model CDR-1 differential scanning calorimeter with a sample pan of aluminium (diameter 5×3 mm), side of which was rolled up. The conditions of DSC were as follows: sample mass about 1 mg; heating rate 10°C min^{-1}, atmosphere static air; reference sample α-Al_2O_3; thermocouple plate Ni/Cr–Ni/Si. The infrared spectra of the decomposition residues were recorded in KBr discs on a 60 SXR FT-IR spectrometer (Nicolet Co., USA) at 4 cm^{-1} resolution.

In the quantum chemical investigation on $[Pb(NTO)_2\cdot H_2O]$ the PM3 calculation of $[Pb(NTO)_2\cdot H_2O]$ were performed by using MOPAC 6.0 program with our experimental geometry of $[Pb(NTO)_2\cdot H_2O]$ as starting values. Through fully optimized geometry and SCF iterative calculations, the electron structure and geometry were obtained. The delocalized canonical MOs have been energy localized. All calculations were carried out on a HP-900 computer in the national key laboratory of Nanjing University of Science and Technology.

Results and discussion

Crystal structure

The crystalline salt is monoclinic, and belongs to space group $P2_1/n$ with crystal parameters of a=0.7262(1) nm, b=1.2129(2) nm, c=1.2268(3) nm, β=90.38(2)°, V=1.0806(2) nm^3, Z=4, D_c=2.97 g cm^{-3}, μ=157.83 cm^{-1}, $F(000)$=888. The final R=0.027, R_w=0.027 (unit mass), and $(\Delta/\sigma)_{max}$=0.09.

Table 1 Atom coordinates and isotropic thermal parameters (in nm^2)

Atoms	x	y	z	B_{eq}
Pb	0.1492(4)	0.5926(2)	0.8086(2)	0.01234(5)
Ow	0.1716(7)	0.4032(4)	0.8804(5)	0.020(1)
O11	–0.1672(7)	0.3697(4)	0.9754(4)	0.016(1)
O12	–0.1906(8)	0.7046(5)	0.7277(5)	0.024(1)
O13	–0.4846(8)	0.6911(5)	0.7036(5)	0.026(1)
O21	0.2170(1)	0.8088(5)	0.8049(5)	0.031(1)
O22	0.3817(9)	1.1954(5)	1.0828(5)	0.027(1)
O23	0.3140(1)	1.1717(6)	0.9151(6)	0.062(2)
N11	–0.4409(9)	0.4335(6)	0.9015(5)	0.020(1)
N12	–0.4975(9)	0.5165(6)	0.8349(5)	0.018(1)
N13	–0.1898(8)	0.5236(5)	0.8598(5)	0.013(1)
N14	–0.3405(9)	0.6613(6)	0.7432(5)	0.018(5)
N21	0.2000(1)	0.8638(5)	0.9857(5)	0.022(1)
N22	0.2270(1)	0.9583(6)	1.0437(6)	0.027(2)
N23	0.2860(1)	0.9871(6)	0.8656(5)	0.021(1)
N24	0.3260(1)	1.1384(6)	0.9916(6)	0.024(1)
C11	–0.2530(1)	0.4364(6)	0.9170(6)	0.015(1)
C12	–0.3440(1)	0.4327(6)	0.8137(5)	0.012(1)
C21	0.2320(1)	0.8810(7)	0.8776(6)	0.022(2)
C22	0.2770(1)	1.0248(7)	0.9686(6)	0.022(2)
Hw1	0.1856	0.3768	0.8912	0.04
Hw2	0.1253	0.4704	0.8551	0.04
H11	–0.4589	0.3626	0.9464	0.04
H21	0.1200	0.8055	0.9284	0.04

The obtained atom coordinates, thermal parameters, bond lengths and bond angles are summarized in Tables 1, 2 and 3. The crystal structure and atom labeling are shown in Fig. 1 and the packing of the molecule in crystal lattice is illustrated in Fig. 2.

As shown in Fig. 1, five NTO anions and one water molecule are the ligands of Pb atom. The coordinate bond lengths are between 0.2466 nm–0.3194 nm, so the distorted tetradecahedron has been formed. The five NTO anions can be divided into two types. The NTO anion of O11b C11b N11b N12b C12b N13b is a digear ligand, it is only coordinated to one Pb atom; the others are trigear ligands and they are coordinated to two Pb atoms.

Table 2 Selected bond lengths (in nm)

Atoms	Bond length	Atoms	Bond length
Pb–Ow	0.2466(5)	N11–C11	0.138(1)
Pb–O11a	0.2692(6)	N12–C12	0.1299(9)
Pb–O12	0.2981(6)	N13–C11	0.1351(9)
Pb–O13b	0.3194(6)	N13–C12	0.137(1)
Pb–O21	0.2668(6)	N14–C12	0.142(1)
Pb–O22a	0.3045(7)	N21–N22	0.1363(9)
Pb–N12b	0.2744(6)	N21–C21	0.136(2)
Pb–N13	0.2679(6)	N22–C22	0.128(2)
Pb–N23a	0.2539(6)	N23–C21	0.135(2)
O11–C11	0.1243(9)	N23–C22	0.135(2)
O12–N14	0.1229(9)	N24–C22	0.145(2)
O13–N14	0.1217(9)	Ow–Hw1	0.0482(5)
O21–C21	0.125(1)	Ow–Hw2	0.1186(5)
O22–N24	0.1218(9)	N11–H11	0.1256(7)
O23–N24	0.122(2)	N21–H21	0.1057(7)
N11–N12	0.1359(9)		

As shown in Fig. 2, there are four Pb atoms, eight NTO anions and four water molecules in a crystal lattice of the title complex. It is quite evident that Pb:NTO:H_2O=1:2:1, therefore the molecular formula of the title complex is [$Pb(NTO)_2 \cdot H_2O$].

From the calculations of equations of the planes, we have found that five ligand NTO anions also can be divided into two types according to space place. One is the NTO anions of O1*i* C1*i* N1*i* N2*i* C2*i* N3*i* (*i*=a, b, blank), which are parallel to each other. The NTO anions of O2*j* C2*j* N2*j* N2*j* C2*j* N3*j* (*j*=a, blank) are another type, and they are parallel too. The atoms in first type plane are all coplaner, but in second type plane are not. Because Pb atoms are closely linked by 80% NTO anions of trigear ligand in the title complex, the network crystal structure is formed.

Mechanism of thermal decomposition of [$Pb(NTO)_2 \cdot H_2O$]

The TG-DTG and DSC curves for [$Pb(NTO)_2 \cdot H_2O$] are shown in Fig. 3. The DSC curve of Fig. 3 shows that there are one endothermic and four exothermic processes at temperatures higher than 190°C. The DTG curve of Fig. 3 shows that there are four processes for the thermal decomposition of [$Pb(NTO)_2 \cdot H_2O$]. In Table 4, the initial and final temperatures of the thermal decomposition processes in the DSC and TG-DTG curves, the mass losses observed between these temperatures in the TG-DTG curve and the decomposition products assigned by IR characteristic absorption

Table 3 Selected bond angles (°)

Atoms	Bond angle	Atoms	Bond angle
Ow–Pb–O11a	78.7(2)	O22a–Pb–N13	106.2(2)
Ow–Pb–O12	126.6(2)	O22a–Pb–N23a	56.9(2)
Ow–Pb–O13b	116.1(2)	N12b–Pb–N13	136.7(2)
Ow–Pb–O21	155.5(2)	N12b–Pb–N23a	75.6(3)
Ow–Pb–O22a	135.3(2)	N13–Pb–N23a	102.4(3)
Ow–Pb–N12b	65.5(2)	N12–N11–C11	111.1(6)
Ow–Pb–N13	71.6(2)	N11–N12–C12	102.5(6)
Ow–Pb–N23a	79.5(2)	C11–N13–C12	103.9(6)
O11–Pb–O12	106.6(2)	O12–N14–O13	124.1(7)
O11a–Pb–O13b	107.4(2)	O12–N14–C12	118.0(6)
O11a–Pb–O21	80.9(2)	O13–N14–C12	117.9(6)
O11a–Pb–O22a	146.0(2)	N22–N21–C21	110.8(6)
O11a–Pb–N12b	84.4(2)	N21–N22–C22	101.3(6)
O11a–Pb–N13	82.1(2)	C21–N23–C22	101.9(6)
O11a–Pb–N23a	155.0(2)	O22–N24–O23	122.9(7)
O12–Pb–O13b	112.6(2)	O22–N24–C22	118.5(7)
O12–Pb–O21	72.5(2)	O23–N24–C22	118.7(8)
O12–Pb–O22a	56.9(2)	O11–C11–N11	123.6(7)
O12–Pb–N12b	164.5(2)	O11–C11–N13	129.7(7)
O12–Pb–N13	57.3(2)	N11–C11–N13	106.6(6)
O12–Pb–N23a	96.2(2)	N12–C12–N13	115.9(6)
O13b–Pb–O21	58.1(2)	N12–C12–N14	121.4(6)
O13b–Pb–O22a	62.4(2)	N13–C12–N14	122.7(6)
O13b–Pb–N12b	52.6(2)	O21–C21–N21	124.7(7)
O13b–Pb–N13	168.6(2)	O21–C21–N23	127.7(7)
O13b–Pb–N23a	71.9(2)	N21–C21–N23	107.6(7)
O21–Pb–O22a	66.1(2)	N22–C22–N23	118.5(8)
O21–Pb–N12b	99.2(3)	N22–C22–N24	121.9(8)
O21–Pb–N13	118.7(3)	N23–C22–N24	119.7(7)
O21–Pb–N23a	116.5(3)	Hw1–Ow–Hw2	92.1(7)
O22a–Pb–N12b	107.9(2)		

Table 4 Mass losses, temperature ranges and decomposition products for $[Pb(NTO)_2 \cdot H_2O]$

DSC		TG-DTG				Decomposition product	IR characteristic absorption/cm^{-1}
Decomp. process	T_{range}/°C	Decomp. process	T_{range}/°C	Mass loss/%			
				experimental	theory		
1	191.0–196.5	I	192–209	3.8	3.7	$Pb(NTO)_2$	1517, 1308, 3390, 1632, 1548, 1382
2	196.5–229.5	II	209–240	26.8		$Pb(OCN)_2$ $PbCO_3$	2151, 1174, 1463, 775
3	229.5–289.3	III	240–322	40.5		$Pb(OCN)_2$ $PbCO_3$ poymers cont. –CO–NH– group	2197, 1172 1461, 772 3407, 1618, 1557, 1385
4	326.8–376.0	IV	322–600	55.5	53.8	PbO	430
5	376.0–419.8					PbO	430

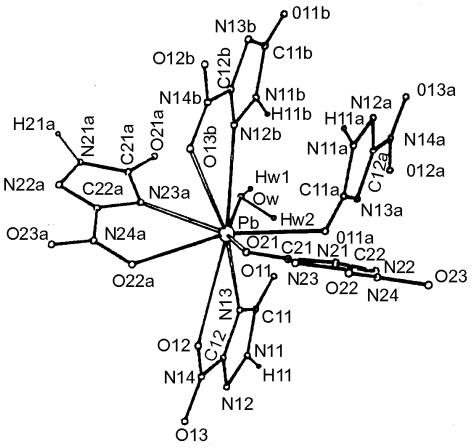

Fig. 1 Crystal structure of $[Pb(NTO)_2 \cdot H_2O]$

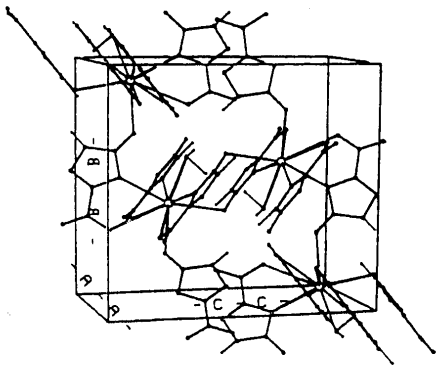

Fig. 2 Packing of the molecular $[Pb(NTO)_2 \cdot H_2O]$ in the crystal lattice

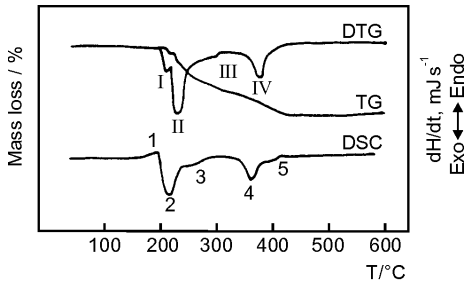

Fig. 3 TG-DTG and DSC curves for $[Pb(NTO)_2 \cdot H_2O]$ at a heating rate of 10°C min^{-1}

peaks are given. It can be seen from Fig. 3 and Table 4 that process 1 (or I) results in a loss of one water molecule. Further decomposition of the dehydrated salt $Pb(NTO)_2$ would occur on heating. The decomposition products for the processes 2 and 3 (or II and III) are a mixture composed of $Pb(OCN)_2$, $PbCO_3$ and polymers containing the –CO–NH– group. The amount of each component can not be determined from the present experiments and it is impossible to determine the decomposition change stoichiometrically. The characteristic absorption peak of the residue formed for the process 5 (or IV) at 430 cm^{-1} is assigned to PbO. At the end of this process, the residue amounted to 44.5%, which is in agreement with the calculated value of 46.2%.

On the bases of experimental and calculated results, the thermal decomposition mechanism of $[Pb(NTO)_2 \cdot H_2O]$ is postulated to be as follows:

$$[Pb(NTO)_2 \cdot H_2O] \xrightarrow[192-209^{\circ}C]{-H_2O} Pb(NTO)_2 \xrightarrow[209-322^{\circ}C]{-NO_2}$$

$$Pb(OCN)_2 + PbCO_3 + \text{polymers} \xrightarrow[322-600^{\circ}C]{} PbO$$

Lattice enthalpy and energy of $[Pb(NTO)_2 \cdot H_2O]$, $\Delta H_L^o[Pb(NTO)_2 \cdot H_2O, cr]$, $\Delta U_L^o[Pb(NTO)_2 \cdot H_2O, cr]$

Setting $\Delta H_L^o[Pb(NTO)_2 \cdot H_2O, cr]$ as the lattice enthalpy in the crystal $[Pb(NTO)_2 \cdot H_2O]$ from $Pb^{2+}(g)$, $NTO^-(g)$ and $H_2O(g)$ at 298.15 K, and $\Delta U_L^o[Pb(NTO)_2H_2O, cr]$ as the crystal lattice energy

$$Pb^{2+}(g) + 2NTO^-(g) + H_2O(g) \xrightarrow{\Delta H_L^o[Pb(NTO)_2 \cdot H_2O, cr]} [Pb(NTO)_2 \cdot H_2O(cr)] \quad (1)$$

we have

$$\Delta H_L^o[Pb(NTO)_2 \cdot H_2O, cr] = \Delta_f H_m^o[Pb(NTO)_2 \cdot H_2O, cr, 298.15\ K] - \Delta_f H_m^o(Pb^{2+},g) - 2\Delta_f H_m^o(NTO^-,g) - \Delta_f H_m^o(H_2O,g) \quad (2)$$

and

$$\Delta U_L^o[Pb(NTO)_2 \cdot H_2O, cr] = \Delta H_L^o[Pb(NTO)_2 \cdot H_2O, cr] - \Delta nRT \quad (3)$$

where $\Delta_f H_m^o[Pb(NTO)_2 \cdot H_2O, cr, 298.15\ K] = -(247.4 \pm 5.9)$ kJ mol^{-1} [8]; $\Delta_f H_m^o(Pb^{2+},g) = 2373.4$ kJ mol^{-1} [9]; $\Delta_f H_m^o(NTO^-,g) = -374.3$ kJ mol^{-1} [10]; $\Delta_f H_m^o(H_2O,g) = -241.82$ kJ mol^{-1} [9]; $\Delta n = -4$; $RT = 2.5$ kJ mol^{-1}.

By substituting the above-mentioned data into Eqs (2) and (3), the following values are obtained:

$$\Delta H_L^o[Pb(NTO)_2 \cdot H_2O, cr] = -1630.4 \text{ kJ mol}^{-1}$$

$$\Delta U_L^o[Pb(NTO)_2 \cdot H_2O, cr] = -1620.4 \text{ kJ mol}^{-1}$$

Lattice energy, lattice enthalpy and standard enthalpy of formation of $Pb(NTO)_2$(cr), $\Delta U_L^o[Pb(NTO)_2, cr]$, $\Delta H_L^o[Pb(NTO)_2, cr]$, $\Delta_f H_m^o[Pb(NTO)_2, cr, 298.15\ K]$

The value of $\Delta U_L^o[Pb(NTO)_2, cr]$ of – 1767 kJ mol^{-1} is obtained using Kapustinskii's equation [11]:

$$\Delta U_L^o = 1201.6 \frac{\eta_1 \eta_2 \sum n'}{\gamma_1 + \gamma_2} \left(1 - \frac{0.345}{\gamma_1 + \gamma_2}\right) \text{kJ mol}^{-1} \quad (4)$$

where η_1 and η_2 are the module of anion and cation charges; n' is the number of ions in the molecule; γ_1 and γ_2 are the radii of anion and cation in Å. For $Pb(NTO)_2$(cr), $\eta_1=\eta_{NTO}=1$; $\eta_2=\eta_{Pb^{2+}}=2$; $n'=n(Pb^{2+}+nNTO^-)=1+2=3$, $\gamma_1=\gamma(NTO^-,g)=2.5$ Å [12]; $\gamma_2=\gamma(Pb^{2+},g)=1.2$ Å.

The values of $\Delta H_L^o[Pb(NTO)_2, cr]$ and $\Delta_f H_m^o[Pb(NTO)_2, cr, 298.15\ K]$ are calculated according to the process (5) and relationships (6) and (7):

$$Pb^{2+}(g) + 2NTO^-(g) \xrightarrow{\Delta H_L^o[Pb(NTO)_2, cr]} Pb(NTO)_2(cr) \quad (5)$$

$$\Delta H_L^o[Pb(NTO)_2, cr] = \Delta U_L^o[Pb(NTO)_2, cr] + \Delta nRT \quad (6)$$

$$\Delta_f H_m^o[Pb(NTO)_2, cr, 298.15\ K] = \Delta_f H_m^o(Pb^{2+},g) + 2\Delta_f H_m^o(NTO^-,g) + \Delta H_L^o[Pb(NTO)_2, cr] \quad (7)$$

where $\Delta U_L^o[Pb(NTO)_2, cr]$=–1767 kJ mol^{-1}; Δn=–3; RT=2.5 kJ mol^{-1}; $\Delta_f H_m^o(Pb^{2+},g)$ =2373.4 kJ mol^{-1} [9]; $\Delta_f H_m^o(NTO^-,g)$=–374.3 kJ mol^{-1} [10].

By substituting the above-mentioned data into Eqs (5), (6) and (7), the following values are obtained:

$$\Delta H_L^o[Pb(NTO)_2, cr] = -1775 \text{ kJ mol}^{-1};$$

$$\Delta_f H_m^o[Pb(NTO)_2, cr, 298.15\ K] = -150.2 \text{ kJ mol}^{-1}.$$

Quantum chemical calculations

Table 5 shows the calculated and experimental bond lengths and angles. Table 6 lists energy levels and compositions of parts of energy-localized MOs. The Wiberg bond [13] orders between atoms in NTO ring are shown in Fig. 4.

From Table 5 we can see that compared with X-diffraction experimental values, the calculated bond lengths and angles of heavy atoms change little with a range of 0.003 nm and 2.2° on average respectively, while those of hydrogen containing bonds vary greatly. For example, the distance Ow–Hw1 increases 0.0470 nm from 0.0482 to 0.0952 nm and bond angle Hw1–Ow–Hw2 increases 15.2° from 92.1 to 107.3°. X-ray method cannot give accurate position for hydrogen atoms. For in-

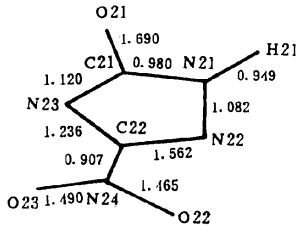

Fig. 4 Wiberg bond order between atoms of a ring

stance, the experimental bond lengths for O–H (0.0482 and 0.1186 nm) and N–H (0.1256 nm) are unreasonable, while calculated results are in good agreement with the covalent lengths (about 0.1 nm).

Table 5 Comparison of some bond lengths and bond angles between observed and calculated values*

Bond length	L1	L2	Bond angle	Ang 1	Ang 2
N11–N12	0.1359	0.1394	N11–C11–N13	106.6	106.2
N11–C11	0.1380	0.1444	N12–N11–C11	111.1	107.6
N12–C12	0.1299	0.1346	N11–N12–C12	102.5	106.2
N13–C11	0.1351	0.1408	C11–N13–C12	103.9	106.0
N13–C12	0.1370	0.1383	O12–N14–C12	118.0	119.4
N14–C12	0.1420	0.1481	O11–C11–N11	123.6	124.0
O11–C11	0.1234	0.1246	O11–C11–N13	129.7	129.7
O12–N14	0.1229	0.1219	N12–C12–N13	115.9	113.5
O13–N14	0.1217	0.1218	N12–C12-N14	121.4	122.3
N11–H11	0.1256	0.0993	N13-C12-N14	122.7	124.1
Ow–Hw1	0.0482	0.0952	Hw1–Ow–Hw2	92.1	107.3
Ow–Hw2	0.1186	0.0970	O12–N14–O13	124.1	119.6
			O13–N14–C12	117.9	120.9

*: L1, L2, Ang1 and Ang2 refer to experimental and calculated bond lengths and bond angles, respectively

From 125 occupied MOs we pick up those 6 MOs in which the AO coefficients of the Pb atom are larger than 0.100 and have adaptable symmetry with corresponding AOs of ligands. The levels and compositions of the 6 MOs are listed in Table 5. It can be seen that Pb atom bonds to ligands only with its *p*-type AOs. Electrons in 6s orbital are lone pair and do not bond to any ligands. Energy level of a bonding MO can indicate the strength of a bond. Comparing levels of MOs, we can find that nitrogen atoms combine more strongly with lead atom than oxygen atoms, so all NTO rings in crystal combine with Pb atoms more strongly than water. When

Table 6 Levels (eV) and compositions of energy-localized bonding MOs

	MO	69	70	71	90	91	114
	(level)	(–9.595)	(–9.588)	(–9.435)	(–7.819)	(–7.732)	(–5.676)
Pb	$6p_x$					0.236	
	$6p_y$		–0.174	–0.229			–0.103
	$6p_z$	0.245	0.122		–0.101		
	AO/ligand	N23a	N12b	N13	O12	Ow	O21
	2s	–0.802	–0.816	0.810	–0.163	0.280	–0.157
	$2p_x$				–0.817	–0.921	–0.585
	$2p_y$	–0.200	0.408	0.471			0.659
	$2p_z$	–0.484	–0.333	–0.231	0.5096		–0.349

$[Pb(NTO)_2 \cdot H_2O]$ is heated, ligand water will be dissociated from it first, which is consistent with the experiment fact [7].

From the Wiberg bond orders between atoms of NTO ring in Fig. 3, we can see that among all bond orders the bond order of C22–N24 bond is the smallest (0.907) and the next smaller one is C21–N21 (0.980). The small bond order indicates that the electron density between the atoms are small, so the bond is relatively weaker. It can be predicted that it is easy to break C22–N24 bond to lose $–NO_2$ and then C21–N21 will also be broken. These theoretical predictions are consistent with experimental facts [7].

References

1 K. Y. Lee, L. B. Chapman and M. D. Coburn, J. Energetic Mater., 5 (1987) 27.
2 E. F. Rothgery, D. E. Audette and R. C. Wedlich, Thermochim. Acta, 185 (1991) 235.
3 L. D. Redman and R. J. Spear, AD-A220339, (1989).
4 X. Yi, H. Rongzu, W. Xiyou, F. Xiayun and Z. Chunhua, Thermochim. Acta, 189 (1991) 283.
5 Z. Tonglai, H. Rongzu, L. Fuping, C. Li and Y. Kaibei, Chinese Science Bulletin, 38 (6) (1993) 523.
6 Z. Tonglai, H. Rongzu, L. Fuping, C. Li and Y. Kaibei, Energetic Materials, 1(1) (1993) 37.
7 Z. Tonglai, H. Rongzu, L. Fuping and Y. Kaibei, Acta Chimica Sinica, 52(6) (1994) 545.
8 M. Zihui and H. Rongzu, J. Therm. Anal., 45 (1995) 79.
9 R. C. Weast, CRC Handbook of Chemistry and Physics, 70th edn, CRC Press Inc., Boca Raton, FL, (1989), D51 93.
10 H. Rongzu, M. Zihui and K. Bing, Thermochim. Acta, 275 (1993) 17.
11 A. F. Kapustinskii, Quent. Rev., 10 (1956) 283.
12 A. Finch, P. J. Gardner, A. J. Head and H. S. Majdi, Thermochim. Acta, 213 (1993) 17.
13 K. B. Wiberg, Tetrahedron, 24 (1968) 1083.